Characterization of Color Printers Using Robust Parameter Estimation

Carlos Lana and Mario Rotea
Purdue University
West Lafayette, IN 47907
clana@purdue.edu, rotea@purdue.edu

Daniel Viassolo
Wilson Center for Research &Technology
Xerox Corp., Webster, NY 14580
dviassolo@ieee.org

Abstract

Colorimetric models are used to predict printer output colors from a set of toner control values. One such a model is the Neugebauer model, which predicts the spectral reflectance of the printed colors. This paper presents a new method for estimating the parameters (dot growth functions and primary reflectances) of the Neugebauer model from a set of measured spectral reflectances. Using information on the size of the uncertainty, a robust estimation algorithm (REA) is proposed to obtain a model with low sensitivity to undesirable and unpredictable variations and uncertainty. A case study using a high-end color printer shows that REA is consistently more robust than existing methods.

1. Introduction

Printer calibration plays a central role in print quality assurance. Calibration is intended to guarantee that a given printer will consistently output the "right colors," despite component aging and toner variation. A characterization, or a model, of the color printer is required as a first step for most calibration methods [13, 4]. Once available, this model is inverted so that the digital control values (the printer inputs) can be calculated as a function of the desired output color.

Techniques for printer characterization can be grouped in two categories: model-based approach, and empirical or interpolation-based approach. The interpolation-based approach has the potential of being more accurate [6, 5] if a large enough number of experiments is available. The model-based approach takes advantage of the physics behind the process to achieve accuracy even in areas of the color space where experimental data is sparse [1, 2, 10, 13].

The present paper considers the characterization of digital color printers using the model-based approach. In particular, this work uses the spectral Neugebauer model [12]. The parameters of this model are usually determined from spectral measurements of the printed colors. Several important papers, e.g. [10, 2, 1, 13], have used this approach to develop or survey algorithms for parameter estimation. Spatial nonuniformities and color drifts may give different characterizations of the same printer depending on when and where on the paper the samples are taken. To our knowledge, the available techniques do not account for these variations as they do not utilize any prior information on uncertainty associated with the measured reflectances.

This work introduces a mathematical framework that explicitly incorporates uncertainty information in the estimation of the model parameters. The notion of worst-case spectral approximation error is introduced, and a closed form expression for evaluating this error is given. We propose to obtain parameter estimates by minimizing the largest worst-case error over all available experiments. The robust estimation algorithm (REA) is developed to solve this optimization problem. A specific estimation problem is solved for a high-end xerographic printer. The model obtained with REA is compared with the ones from two other algorithms based on least squares and total least squares [13]. This comparative analysis suggests that REA yields the most robust model.

Notation

r_o	True (unknown) reflectance
$\hat{r}$	Model output reflectance
$\hat{r}_P$	Model primary reflectance.
r	Measured reflectance
r_C, r_M, r_Y, r_K	Cyan, magenta, yellow, and black single colorant measured reflectances
C, M, Y, K	Cyan, Magenta, Yellow, and Black digital control values
c, m, y, k	Cyan, magenta, yellow and black nondimensional actual areas
w	Neugebauer area
λ	Wavelength
σ	Reflectance error bound
$\mathcal{R}_o$	Reflectance uncertainty set

2. The Neugebauer Printer Model

In this paper we consider four-colorant printers modeled by the spectral Neugebauer equation studied in [9, 11, 12]

and given by

$$\hat{r}(\lambda) = \left\{ \sum_{i=1}^{16} w_i \hat{r}_{P,i}^{1/n}(\lambda) \right\}^n \quad (1)$$

where $\hat{r}(\lambda)$ is the output reflectance at wavelength λ predicted by the model, w_i is a positive weight representing the so-called Neugebauer primary area, $\hat{r}_{P,i}(\lambda)$ denotes the best available estimate for the i^{th} primary reflectance, and the number n is the Yule-Nielsen correction factor. See reference [12] for further details on this model. For printers using rotated halftone screens, the Neugebauer areas can be modeled with the so-called Demichel equations (2)

$$\begin{aligned}
w_1 &= (1-c)(1-m)(1-y)(1-k) && (2a)\\
w_2 &= c(1-m)(1-y)(1-k) && (2b)\\
w_3 &= (1-c)m(1-y)(1-k) && (2c)\\
w_4 &= (1-c)(1-m)y(1-k) && (2d)\\
w_5 &= (1-c)(1-m)(1-y)k && (2e)\\
w_6 &= cm(1-y)(1-k) && (2f)\\
w_7 &= c(1-m)y(1-k) && (2g)\\
w_8 &= c(1-m)(1-y)k && (2h)\\
w_9 &= (1-c)my(1-k) && (2i)\\
w_{10} &= (1-c)m(1-y)k && (2j)\\
w_{11} &= (1-c)(1-m)yk && (2k)\\
w_{12} &= cmy(1-k) && (2l)\\
w_{13} &= cm(1-y)k && (2m)\\
w_{14} &= c(1-m)yk && (2n)\\
w_{15} &= (1-c)myk && (2o)\\
w_{16} &= cmyk && (2p)
\end{aligned}$$

where c, m, y and k are the nondimensional actual areas occupied by cyan, magenta, yellow and black toner, respectively. Theses areas are determined by the digital control values C, M, Y and K, which are nondimensional integers from 0 to 255 used to "tell the printer" how much cyan, magenta, yellow and black toner needs to be placed on the paper.

Figure 1 depicts the input-output printer model composed by equation (1), the Demichel equations (2), and the dot growth functions $C \mapsto c, M \mapsto m, Y \mapsto y$, and $K \mapsto k$. For the model to be fully specified the following need to be known: **(1)** the dot growth functions $C \mapsto c, M \mapsto m, Y \mapsto y$, and $K \mapsto k$; **(2)** the model primary reflectances $\hat{r}_{P,1}(\lambda)$, ..., $\hat{r}_{P,16}(\lambda)$; **(3)** the Yule-Nielsen factor n. These parameters may be determined in the following three steps

1. Measure all 16 primary reflectances $r_{P,1}, \ldots, r_{P,16}$
2. Run a predefined set of input-output experiments, where the reflectances $r(\lambda)$ of color patches printed in response to known digital control input values C, M, Y, K are measured
3. Determine samples of the dot growth functions c, m, y, k, the Yule-Nielsen factor n, and (optionally) the corrected primary reflectances by minimizing a suitable measure of modeling error.

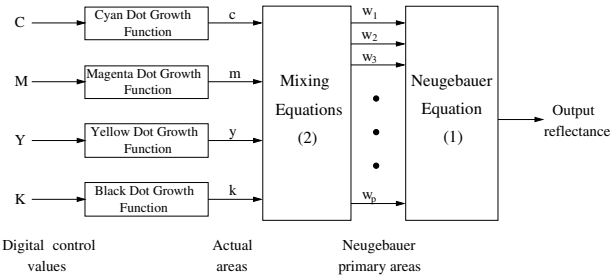

Figure 1: *Input-output model for a color printer*

3. The Worst-Case Modeling Error

Let

$$\|x\|_2 = \sqrt{\sum_{k=1}^{N} x_k^2}$$

denote the ℓ_2 norm of the sequence $x = (x_1, \ldots, x_N)$. Suppose that the printer model in Figure 1 is known, and let $r_o = (r_o(\lambda_1), \ldots, r_o(\lambda_N))$ denote the true (generally unknown) output reflectance sequence (at wavelengths λ_1, ..., λ_N) in response to known inputs C, M, Y, K. The ℓ_2 *model approximation error* E is defined as

$$E = \|\hat{r} - r_o\|_2 \quad (3)$$

where $\hat{r} = (\hat{r}(\lambda_1), \ldots, \hat{r}(\lambda_N))$ is the output reflectance sequence obtained from the model in equation (1).

The error E is unknown. Thus, a natural measure of model performance is the *worst-case approximation error* E_{worst} defined by

$$E_{\text{worst}} = \max_{r_o \in \mathcal{R}_o} \|\hat{r} - r_o\|_2 \quad (4)$$

where $\mathcal{R}_o$ is a known set containing the true output reflectance r_o, which we now define as

$$\mathcal{R}_o = \{r_o \text{ s.t. } \sigma^-(\lambda_k) \le r_o(\lambda_k) - r(\lambda_k) \le \sigma^+(\lambda_k) \quad \forall k = 1, \ldots, N\} \quad (5)$$

where $\sigma^-(\lambda_k)$ and $\sigma^+(\lambda_k)$ are given lower and upper error bounds at wavelength λ_k. The following result gives a closed-form expression to compute the worst-case error in (4).

Proposition 1 ([8]) *With $\mathcal{R}_o$ given by (5), the worst-case approximation error defined in (4) satisfies*

$$E_{\text{worst}} = \left\| \left| \hat{r} - r - \frac{\sigma^+ + \sigma^-}{2} \right| + \frac{\sigma^+ - \sigma^-}{2} \right\|_2 \quad (6)$$

where $\sigma^- = (\sigma^-(\lambda_1), \sigma^-(\lambda_2), \ldots, \sigma^-(\lambda_N))$ and $\sigma^+ = (\sigma^+(\lambda_1), \sigma^+(\lambda_2), \ldots, \sigma^+(\lambda_N))$ are the lower and upper bound sequences; $r = (r(\lambda_1), r(\lambda_2) \ldots, r(\lambda_N))$ is the measured reflectance sequence; and $\hat{r} = (\hat{r}(\lambda_1), \hat{r}(\lambda_2) \ldots, \hat{r}(\lambda_N))$ is the model output reflectance sequence computed using (1).

4. Printer Modeling Via Minimization Of Worst-Case Errors

This section describes how to obtain a printer model that attempts to minimize the worst-case error in (6) over a set of multiple experiments. The experimental data necessary for this analysis is listed first, followed by a summary of the model parameters to be estimated and the cost function to be optimized.

Primary reflectances The measured primary reflectance sequences are denoted by

$$r_{P,j} = (r_{P,j}(\lambda_1), \ldots, r_{P,j}(\lambda_N)) \tag{7}$$

where $j = 1, \ldots, 16$, indexes the specific reflectance and $\lambda_1, \ldots, \lambda_N$, are the wavelengths of interest. These reflectances are obtained in response to all 16 possible combinations of control inputs C, M, Y, K where each control value is either 0 or 255.

Responses to single colorant inputs The measured output reflectance sequences in response to a set of single colorant digital control values C, M, Y, K, are denoted by

$$r_{C,j} = (r_{C,j}(\lambda_1), \ldots, r_{C,j}(\lambda_N)) \tag{8a}$$
$$r_{M,j} = (r_{M,j}(\lambda_1), \ldots, r_{M,j}(\lambda_N)) \tag{8b}$$
$$r_{Y,j} = (r_{Y,j}(\lambda_1), \ldots, r_{Y,j}(\lambda_N)) \tag{8c}$$
$$r_{K,j} = (r_{K,j}(\lambda_1), \ldots, r_{K,j}(\lambda_N)) \tag{8d}$$

where the subindex C, M, Y, or K represent the reflectance obtained in response to digital control values of the form $(C, 0, 0, 0)$ (cyan only), $(0, M, 0, 0)$ (magenta only), $(0, 0, Y, 0)$ (yellow only), $(0, 0, 0, K)$ (black only), respectively. The subindex j is an integer that denotes the experiment number and it runs from 1 to Q.

Responses to multicolorant inputs To obtain a good representation of the input color space, colors combining C, M, Y and K are also included. We denote the measured output reflectance sequences of these colors by

$$r_j = (r_j(\lambda_1), \ldots, r_j(\lambda_N)) \tag{9}$$

where $j = 1, \ldots, L$ and L denotes the number of multicolorant experiments.

Uncertainty bounds The uncertainty bounds were introduced in equation (5). They are denoted by

$$\sigma_j^+ = (\sigma_j^+(\lambda_1), \ldots, \sigma_j^+(\lambda_N)) \tag{10a}$$
$$\sigma_j^- = (\sigma_j^-(\lambda_1), \ldots, \sigma_j^-(\lambda_N)) \tag{10b}$$

where the subindex j indicates the reflectance sequence under consideration.

Model parameters The model parameters to be estimated using the previously described data are: the four dot growth functions $C \mapsto c$, $M \mapsto m$, $Y \mapsto y$, $K \mapsto k$, the corrected primary reflectance sequences $\hat{r}_{P,1}$, ..., $\hat{r}_{P,16}$, and the Yule-Nielsen correction factor n.

Ideal problem We would like to obtain the model parameters that minimize the worst-case approximation error over the experimental data. That is, to minimize the cost function

$$\max_j E_{\text{worst},j} \tag{11}$$

where $E_{\text{worst},j}$ is the worst-case approximation error calculated from (6), using the measured primary reflectances $r_{P,j}$ in (7), the measured reflectances (8) or (9) depending on the index j, and the bounds in (10).

5. The Robust Estimation Algorithm (REA)

The ideal minimization problem defined above involves a joint search for the actual areas (the dot growth functions) and the primary reflectances. This is a difficult nonconvex search with local optima that may not be global. This section describes an algorithm to compute a suboptimal solution to this problem by splitting it into two simpler problems: the estimation of the dot growth functions and the estimation of the corrected primary reflectances, both problems with constant n. These problems are simpler because they do not involve products amongst the optimization variables.

5.1. Estimation of dot growth functions

For the set of single colorant control values, the nonlinear Demichel equations (2) become an affine relation between the Neugebauer areas $w_1, w_2, \ldots, w_{16}$ and the actual areas c, m, y, k. Therefore, the model reflectances for single colorant inputs are simplified to the following

Digital Control Values	Reflectance	
$C = C_j, M = Y = K = 0$	$\hat{r}_{C,j} = \left\{(1 - c_j)\hat{r}_{P,1}^{1/n} + c_j\, \hat{r}_{P,2}^{1/n}\right\}^n$	(12a)
$M = M_j, C = Y = K = 0$	$\hat{r}_{M,j} = \left\{(1 - m_j)\hat{r}_{P,1}^{1/n} + m_j\, \hat{r}_{P,3}^{1/n}\right\}^n$	(12b)
$Y = Y_j, C = M = K = 0$	$\hat{r}_{Y,j} = \left\{(1 - y_j)\hat{r}_{P,1}^{1/n} + y_j\, \hat{r}_{P,4}^{1/n}\right\}^n$	(12c)
$K = K_j, C = M = Y = 0$	$\hat{r}_{K,j} = \left\{(1 - k_j)\hat{r}_{P,1}^{1/n} + k_j\, \hat{r}_{P,5}^{1/n}\right\}^n$	(12d)

It follows from equation (12) that the minimization of the largest worst-case error over the actual areas decouples into the following subproblems

$$c_j = \arg\min_{c_j \in [0,1]} \left\| \left| \hat{r}_{C,j} - r_{C,j} - \frac{\sigma_j^+ + \sigma_j^-}{2} \right| + \frac{\sigma_j^+ - \sigma_j^-}{2} \right\|^2 \quad (13a)$$

$$m_j = \arg\min_{m_j \in [0,1]} \left\| \left| \hat{r}_{M,j} - r_{M,j} - \frac{\sigma_j^+ + \sigma_j^-}{2} \right| + \frac{\sigma_j^+ - \sigma_j^-}{2} \right\|^2 \quad (13b)$$

$$y_j = \arg\min_{y_j \in [0,1]} \left\| \left| \hat{r}_{Y,j} - r_{Y,j} - \frac{\sigma_j^+ + \sigma_j^-}{2} \right| + \frac{\sigma_j^+ - \sigma_j^-}{2} \right\|^2 \quad (13c)$$

$$k_j = \arg\min_{k_j \in [0,1]} \left\| \left| \hat{r}_{K,j} - r_{K,j} - \frac{\sigma_j^+ + \sigma_j^-}{2} \right| + \frac{\sigma_j^+ - \sigma_j^-}{2} \right\|^2 \quad (13d)$$

where $\hat{r}_{C,j}$, $\hat{r}_{M,j}$, $\hat{r}_{Y,j}$, and $\hat{r}_{K,j}$, for $j = 1, \ldots, Q$, are the model output reflectance sequences computed using (12), and $r_{C,j}$, $r_{M,j}$, $r_{Y,j}$, and $r_{K,j}$ are the measured reflectance sequences corresponding to single colorant inputs defined in (8). This result follows from the fact that the minimization of the maximum of a set of functions of independent variables is equal to the maximum of the set containing the minimum of those functions. See [8] for further details.

5.2. Estimation of corrected primary reflectances

Considering the dot-growth functions and the Yule-Nielsen factor fixed, the estimation of the corrected primary sequences $\hat{r}_{P,i}$, for $i = 1, \ldots, 16$, can be obtained by minimizing the largest worst-case error in (11) over the set of primary sequences consistent with the measurements. More precisely, the corrected primary sequences can be obtained from

$$[\hat{r}_{P,1}, \ldots, \hat{r}_{P,16}] = \arg\min \max_j \left\| \left| \hat{r}_j - r_j - \frac{\sigma_j^+ + \sigma_j^-}{2} \right| + \frac{\sigma_j^+ - \sigma_j^-}{2} \right\|^2 \quad (14)$$
$$\text{s.t. } \hat{r}_{P,1} \in \mathcal{R}_{o,1}, \ldots, \hat{r}_{P,16} \in \mathcal{R}_{o,16}$$

where $\hat{r}_j$ is the model output reflectance sequence calculated using equation (1) with Neugebauer areas computed from the Demichel equations (2) and the given dot growth functions. In (14), r_j is the measured reflectance corresponding to single or multicolorant responses in (8) or (9), respectively, and the bounds σ_j^- and σ_j^+ in (10) corresponding to the measured reflectance r_j.

5.3. The robust estimation algorithm (REA)

We summarize our approach in the following robust estimation algorithm (REA):

1. Fix the primary reflectances to the measured sequences (7). Compute Q samples of the dot-growth functions $C \mapsto c$, $M \mapsto m$, $Y \mapsto y$, $K \mapsto k$ by solving the scalar optimization problems defined in equation (13).

2. Set the dot-growth functions to the ones computed in step 1 and compute N samples of the corrected primary reflectances by solving (14).

3. Execute steps 1 and 2 for several values of n to identify the Yule-Nielsen correction factor n that minimizes the largest worst-case approximation error defined in (11).

The parameter estimation could be improved by iterating over steps 1-3. For instance, one could obtain a first estimate of the parameters using REA (steps 1-3) and refine this estimate by applying iteratively REA but now replacing the measured primary reflectances in step 1 with the corrected ones from the previous iteration.

The minimization problems in steps 1 and 2 can be solved using functions from the Matlab Optimization Toolbox 7. The dot growth functions can be computed solving (13) with the Matlab function `fmincon`. The corrected primary reflectances can be computed solving (14) with the Matlab function `fminimax`.

6. Modeling of a high-end xerographic color printer

This section illustrates the REA, and compares it with the least squares (LS) and total least squares (TLS) algorithms presented in [13].

A set of color charts compatible with the LS and TLS methods explained in [13] was generated. Spectral reflectances for parameter estimation and model validation are measured from color patches generated as explained below.

The training data set used for parameter estimation is divided in two subsets of reflectances: the response to single colorant inputs and the response to multicolorant inputs. The single colorant responses use Q=17 single digital control input as shown in (8). The multicolorant responses (9) use 17 values of C, M, Y control inputs ganged together ($C = M = Y$) with $K = 0$, and 17 values of each single control input with the remaining digital control inputs set to mid-range. This gives a total of 153 control values for the training set.

The test set used for model validation consists of 125 control values taken from a homogeneous $5 \times 5 \times 5$ grid in the CMY color space and then converted to the $CMYK$ color space using a standard undercolor removal algorithm. In addition, the responses to 16 control values corresponding to the primary reflectances in equation (7) are also measured.

Patches corresponding to identical control inputs were printed and measured at four different spatial locations on the charts. Reflectances were measured at 10nm intervals between 380nm and 730nm using a Gretag spectrophotometer model SPM50. The reflectances used for parameter estimation and model validation were obtained averaging the four measurements available for each of the control value.

6.1. Printer modeling using REA

A printer model was obtained using the basic REA explained before. The algorithm requires the sequences σ^- and σ^+ defined in (10). Using the four measurements available per control input in the training set, a symmetric bound sequence $\sigma^- = -\sigma^+$ was constructed and used for the computation of the worst-case errors and to constrain the search for corrected primary reflectances as required by (14).

To determine the sequence σ^+ we proceed as follows. First we remove from the measured reflectances the mean of each four-measurement group. We call this data *measurement errors*. Analysis shows that over 90% of the measurement errors have absolute value smaller than twice the standard deviation of the data, which is consistent with a normal-like distribution of the measurement errors. See Figure 2. The error bound sequence σ^+ is taken to be twice the standard deviation of the measurement errors.

The results of step 1 of REA are shown in Figure 3. This figure shows the four dot-growth functions $C \mapsto c$, $M \mapsto m$, $Y \mapsto y$, and $K \mapsto k$. This result is obtained with Yule-Nielsen factor $n = 7.7$, a choice that will be justified later.

Figure 4 shows the first four primary reflectances. The solid lines represent the corrected primaries $\hat{r}_{P,j}$ from step 2 of REA. The dotted lines give the measured primary reflectances $r_{P,j}$. The dashed lines are the limits $r_{P,j} - \sigma^+$ and $r_{P,j} + \sigma^+$ that define the feasible set for the corrected primaries.

The REA was run for different Yule-Nielsen correction factors n to identify the best one. An optimal n minimizes the largest worst-case approximation error defined in (11). From Figure 5 it follows that $n = 7.7$ is optimal.

6.2. Comparison with other methods

This section compares the performance of the model obtained using REA with two other models obtained using least squares (LS) and total least squares (TLS) algorithms [13]. The performance comparisons are done analyzing the distribution (over the experiments) of the worst-case errors. We look at the cumulative distribution of the worst-case error over two different sets of experiments: the training data set and the test data set. We also analyze the distribution of the approximation error when the real (unknown) reflectances are randomly generated.

The LS and TLS models considered below were calculated applying the algorithm in [13] to single and multicolorant responses defined in (8) and (9), respectively. Unlike the results in [13], further primary reflectance estimation was not applied because it requires to have an additional set of experiments not available for this work.

Worst-case approximation errors over the training set

Figure 6 shows the cumulative frequency distribution of the worst-case error E_{worst} computed using equation (6). This plot shows how the worst-case error distributes among the experiments in the training set. The plot shows that REA is the best of all three models when evaluated with the worst-case approximation error on the training set. From Table 1 it follows that REA reduces the largest worst-case error (100^{th} percentile) by 28% and 35% relative to TLS and LS, respectively.

Method	Percentiles		
	50^{th}	75^{th}	100^{th}
LS	0.1226	0.1431	0.1981
TLS	0.1167	0.1312	0.1783
REA	0.1114	0.1213	0.1279

Table 1: *Percentile comparison of the worst-case approximation error with training data*

Worst-case approximation errors over the test set

The robustness of the estimation scheme needs to be demonstrated on validation data that is not used for parameter estimation. The cumulative frequency distribution of the worst-case approximation error with test (validation) data is shown in Figure 7. Table 2 quantifies the comparison. Notice that REA is the best performing model for the 75^{th} percentile and 100^{th} percentile (largest worst-case error over the test data) with reduction of worst-case errors ranging from 3.3% to 9.1% for TLS and LS, respectively.

Method	Percentiles		
	50^{th}	75^{th}	100^{th}
LS	0.1431	0.1739	0.3029
TLS	0.1385	0.1669	0.2844
REA	0.1395	0.1630	0.2751

Table 2: *Percentile comparison of the worst-case approximation error with test data*

Approximation errors

Here we analyze the distribution of approximation errors (not the worst-case) for randomly generated spectral reflectances. The analysis uses 5000 random reflectances for each control value of the training set and 5000 random reflectances for each control value in the test set. These random reflectances are generated from a normal distribution with mean equal to the measured reflectance and standard deviation equal to half the error bound sequence σ^+.

Table 3 shows the percentiles of the approximation error distribution with training and test data. In all cases but one (median with test data) REA has smaller approximation errors than LS and TLS.

Method	Training		Test	
	50^{th}	75^{th}	50^{th}	75^{th}
LS	0.0618	0.0770	0.0783	0.1054
TLS	0.0566	0.0665	0.0736	0.1002
REA	0.0525	0.0600	0.0744	0.0990

Table 3: *Percentile comparison of the approximation error with training and test data*

Approximation errors in the L*a*b* color space

Approximation errors were also computed in the L*a*b* color space[1] using the color difference metric ΔE^*_{ab} [3]. A distribution of ΔE^*_{ab} using random reflectances was generated. Percentiles of the error distribution are shown in Table 4. In all cases, the approximation error with REA is smaller than with LS or TLS.

Method	Percentiles		
	50^{th}	75^{th}	95^{th}
LS	2.36	3.52	5.40
TLS	2.16	3.37	5.24
REA	2.01	3.10	5.15

Table 4: *Percentile comparison of the ΔE^*_{ab} approximation error*

7. Conclusions

A new framework for parameter estimation of printer models has been presented. This framework enables the incorporation of modeling uncertainty into the problem formulation explicitly. We have proposed to measure model quality using the largest approximation error that can take place in spectral space when the measured reflectances are within known limits. A closed form expression for the worst-case approximation error has been given. This expression is readily computed from available data.

A robust parameter estimation algorithm (REA) was presented. This algorithm is based on the idea that the most robust set of parameters is the one that minimizes the worst-case approximation error. This minimization problem is non convex and hard to solve. REA gives a suboptimal solution to this problem by splitting it into two simpler subproblems, the estimation of dot growth functions and the estimation of the corrected primary reflectances.

The results of a case study using a high-end color printer were given. A comparative analysis between REA and existing algorithms based on the least squares and total least squares methods was presented. The analysis of approximation errors (worst-case and otherwise) shows that REA is consistently more robust than LS and TLS in the sense that it achieves the lowest errors over the various data sets.

[1] Reflectances are converted to L*a*b* color space under the CIE iluminant D50

Acknowledgments

This work was supported in part by a Xerox Foundation University Affairs Committee Grant and in part by the National Science Foundation Grant ECS #0080832. The authors are thankful to Prof. Jan Allebach, Purdue University, to Dr. Raja Bala, Xerox Corp., and to Prof. Gaurav Sharma, University of Rochester, for their help.

Biography

Carlos Lana received his B.S. degree in Electronic Engineering from National University of Rosario, Argentina in 2001 and his M.S. degree in Engineering from Purdue University in 2003. He is currently a Ph.D. student at Purdue University. His research interests are in the area of control and optimization. Carlos Lana is member of IEEE Control Systems Society and Professional Communication Society.

Mario Rotea (Contact Author) is a Professor of Aeronautics and Astronautics at Purdue University. He joined the faculty in 1990 after obtaining a PhD degree in Control Science and Dynamical Systems from the University of Minnesota. Dr. Rotea holds degrees in Electrical Engineering from the University of Minnesota (MSEE, 1988) and the National University of Rosario, Argentina (EE diploma, 1983). His research and teaching activities are focused on control engineering and optimization. His group has contributed theory and practical algorithms for performance analysis, parameter estimation, and control of systems with inexact and uncertain models. Dr. Rotea was a Senior Research Engineer with the United Technologies Research Center. In this capacity, he was member of a team responsible for identifying and demonstrating the benefits

of active control and optimization in a diverse set of applications and products. Dr. Rotea is author or co-author of more than 100 technical articles and reports. He is the co-author of SODA and LFTB, which are codes for analysis and optimization of uncertain frequency response functions.

Daniel Viassolo obtained his Ph.D. from Purdue University, with emphasis in control systems, in 2000. From late 1999 until mid 2003, he was a research staff member with Xerox Corp. in Webster, NY. He is now with the Automation & Controls Lab of General Electric Global Research in Niskayuna, NY. He has more than 15 papers published in journals and conference proceedings, and 5 U.S. patent applications.

References

1. R. Balasubramanian. The use of spectral regression in modeling halftone color printers. In *IST/OSA Anual Conference, Optics Imaging in the Information, Age Rochester, NY*, pages 372–375, October 1996.
2. R. Balasubramanian. Optimization of the spectral neugebauer model for printer characterization. *Electronic Imaging*, 8(2):156–166, April 1999.
3. CIE. *Colorimetry*. CIE Publication no. 15.2, Central Bureau of the CIE, Vienna, Austria, 2nd edition, 1986.
4. P. Emmel and R.D. Hersch. Colour calibration for colour reproduction. In *IEEE International Symposium on Circuits and Systems*, pages V105–V108, Geneva, Switzerland, May 2000.
5. J. Hardeberg and F. Schmitt. Color printer characterization using a computational geometry approach. In *IS&T and SID's 5th Color Imaging Conference: Color Science, Systems and Applications*, 1997.
6. P. C. Hung. Colorimetric calibration in electronic imaging devices using a look-up table model and interpolations. *Electronic Imaging*, 2:53–61, January 1993.
7. MathWorks Inc. *Optimization Toolbox User's Guide, version 2.1*. 2000.
8. C. Lana, M. Rotea, and D. Viassolo. Characterization of color printers using robust parameter estimation. *In preparation*, 2003.
9. H.E.J. Neugebauer. Die theoretischen grundlagen des mehrfarbenbuchdrucks. *Zeitschrift fr Wissenshaftliche Photographie Photophysik und Photochemie*, 36:73–89, 1937.
11. R. Rolleston and R. Balasubramanian. Accuracy of various types of neugebauer models. In *IS&T and SID's Color Imaging Conference: Transforms and Transportability of Color*, pages 32–37, Nov. 1993.
11. J. A. S. Viggiano. The color of halftone tints. In *Technical Association of the Graphic Arts (TAGA)*, pages 647–661, 1985.
12. J. A. S. Viggiano. Modeling the color of multi-colored halftones. In *Technical Association of the Graphic Arts (TAGA)*, pages 44–62, 1990.
13. M. Xia, E. Saber, G. Sharma, and M. Tekalp. End-to-end color printer calibration by total least squares regression. *IEEE Transactions on Image Processing*, 8(5):700–716, May 1999.

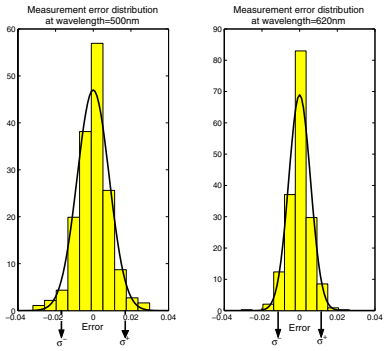

Figure 2: *Distribution of measurement error at $\lambda = 500$nm (left) and $\lambda = 620$nm (right). Bar graph: data. Solid: normal approximation.*

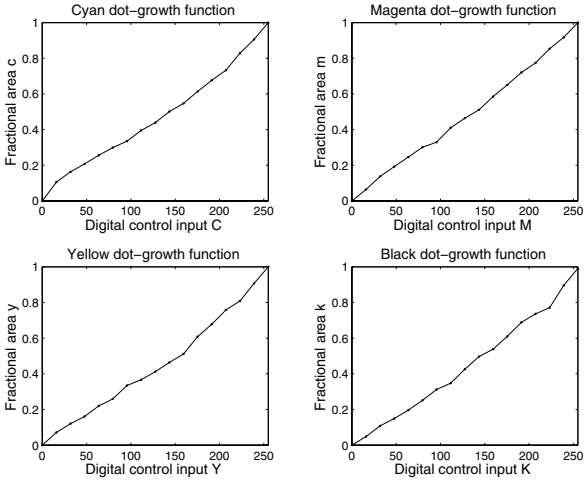

Figure 3: *Dot growth functions obtained using REA, with Q=17 computed samples.*

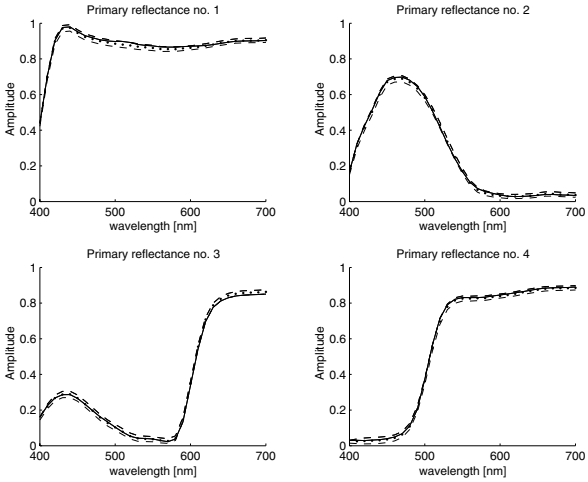

Figure 4: *Primary reflectances no. 1-4. Dotted: measured reflectance. Dashed: bounds. Solid: REA.*

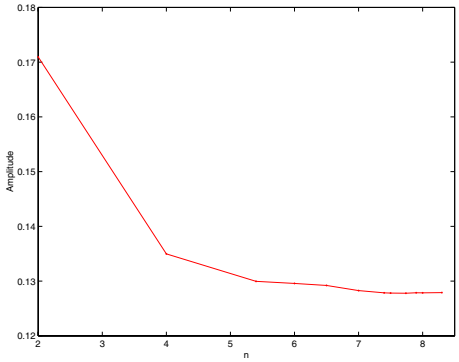

Figure 5: *Largest worst-case error calculated from (11) over the training data set as a function of the Yule-Nielsen factor n.*

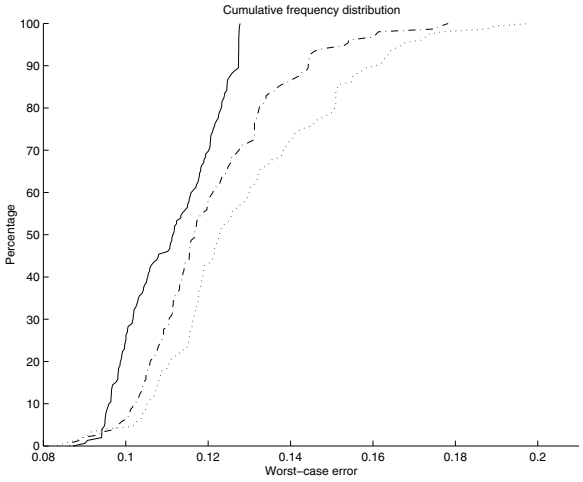

Figure 6: *Cumulative frequency distribution of worst-case approximation errors over the training data set. Solid: REA. Dash-dot: TLS. Dotted: LS.*

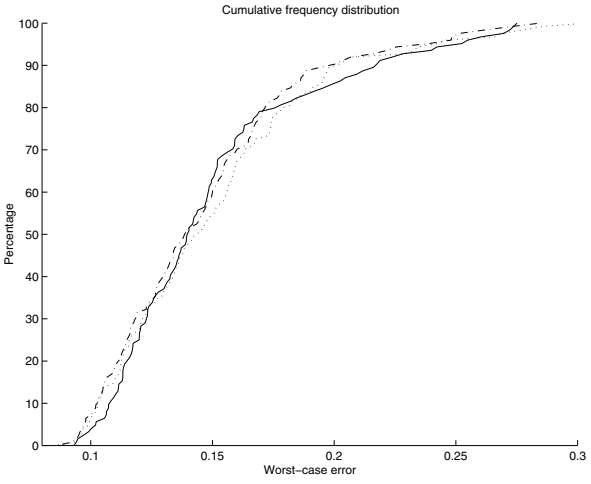

Figure 7: *Cumulative frequency distribution of worst-case approximation errors over the test data set. Solid: REA. Dashdot: TLS. Dotted: LS.*